NASA TECHNICAL NOTE

NASA TN D-3145

COMBINED HIGH-LOW THRUST PROPULSION FOR THE CLOSE SOLAR PROBE MISSION

by William C. Strack

Lewis Research Center
Cleveland, Ohio

NATIONAL AERONAUTICS AND SPACE ADMINISTRATION • WASHINGTON, D. C. • DECEMBER 1965

NASA TN D-3145

COMBINED HIGH-LOW THRUST PROPULSION FOR THE CLOSE SOLAR PROBE MISSION

By William C. Strack

Lewis Research Center
Cleveland, Ohio

NATIONAL AERONAUTICS AND SPACE ADMINISTRATION

For sale by the Clearinghouse for Federal Scientific and Technical Information
Springfield, Virginia 22151 – Price $2.00

COMBINED HIGH-LOW THRUST PROPULSION FOR THE CLOSE SOLAR PROBE MISSION

by William C. Strack

Lewis Research Center

SUMMARY

Several types of propulsion systems are evaluated for the 0.1-AU solar probe mission commencing from a low, circular Earth orbit. The four propulsion systems compared are (1) the chemical rocket, (2) the nuclear rocket, (3) the electric rocket, and (4) the chemical-electric hybrid system. The chemical-electric hybrid system consists of a chemical first stage fired until at least escape velocity is attained and an electrically propelled second stage. For this comparison, calculus of variations calculations were performed upon a mathematical model set up for electric and chemical-electric hybrid systems employing constant-thrust engines.

It is shown that the chemical-electric hybrid is by far the most attractive system for present and near future powerplant technology. In particular, the Saturn IB booster cannot deliver any payload to 0.1 AU if existing (or near future) hardware is utilized regardless of the upper stage propulsion choice except for the chemical-electric hybrid system. The study considers mission times between 60 and 650 days and specific electric powerplant masses from 10 to 150 pounds per kilowatt.

INTRODUCTION

Unquestionably mankind's environment is predominately controlled by the Sun. It is only natural then to increase our scientific knowledge of the "center of attraction" in order to understand and anticipate the behavior of our environment and its underlying mechanisms. At present, our knowledge of the Sun is based almost entirely upon limited experiments performed on Earth. The protective atmospheric and electromagnetic shields surrounding the Earth limit Earth-based solar observations to optical and radio frequencies in the electromagnetic spectrum and severely restrict the study of solar particle emission.

This situation is being alleviated in some degree by orbiting solar observatories and interplanetary probes. There remains, however, a great deal of desirable knowledge that requires a direct close-in study of the Sun (refs. 1 and 2). Requiring a solar probe to attain a perihelion radius of 0.1 AU is justified on the grounds that Sun-probe distances of this magnitude are required by some of the important proposed solar experiments (corona radar sounding, ultraviolet and X-ray spatial resolution of the solar disk, determining the connection between the rotating solar corona and the solar wind, etc.). The intent of this note is not to discuss these experiments or the makeup of the scientific payloads that perform them, but rather to analyze vehicle systems capable of accomplishing this mission - with emphasis on the combined chemical-electric system.

There have been several solar flyby probe studies in the past. The case of high thrust transfers utilizing one or more heliocentric pulses is analyzed in references 3 to 6. The major conclusion from these studies is that only very small payload fractions exist (if any at all) for close solar flybys using chemical propulsion.

An evaluation of the solid-core nuclear rocket for this mission was done in reference 6 for Saturn IB class boosters. Although some payload capability was reported in the study, it must be considered quite optimistic since the tungsten-core nuclear engine was assumed to weigh only about 1400 pounds. (Nerva class engines are about an order of magnitude heavier.) The 5000-pound graphite-core nuclear engine assumed in reference 7 for this mission allowed no payload for Saturn IB class boosters.

The application of a constant-thrust electric propulsion system to this mission has been studied in some degree in references 6 to 8. In all cases, the specific mass of the electric propulsion system was assumed to lie far below present and near future capabilities. Furthermore, the electric stage was assumed to commence either in Earth orbit or at Earth escape, thus avoiding the question of when should chemical propulsion cease and electric propulsion begin.

The present study evaluates constant-thrust electric propulsion in light of both future and present capabilities with regard to powerplant specific mass (values between 10 and 150 lb/kW are assumed). It also investigates the problem of optimum staging between high- and low-thrust stages. In particular, it is assumed that electric propulsion begins either in Earth orbit (designated herein as the electric system) or at some arbitrary velocity following Earth escape (designated herein as the chemical-electric hybrid system).

A comparison between the various systems is then made in terms of payload ratio, mission time, and electric power requirements. The power requirement of the payload is an important parameter for this mission since payload ratios are small and the power required for onboard experiments and telemetry in the vicinity of the Sun can be quite large. Power estimates range from several hundred watts to several kilowatts (ref. 8).

ANALYSIS

No analysis is presented herein for chemical and nuclear systems. Instead, the results of other studies such as reference 7 are used where needed. This analysis is concerned with determining the performance of electric and chemical-electric hybrid systems initially in a 100-nautical-mile circular Earth orbit. Payload ratio will be the primary performance criterion. Actually, mission time and electric power are of importance, too, and an example of the tradeoffs among these three entities will be given in the section RESULTS AND DISCUSSION. The chemical-electric hybrid system is treated first.

Hybrid System

The problem is to determine the maximum payload ratio achievable with a chemical first stage and a constant-thrust electric second stage, holding mission time, specific powerplant mass, and other vehicle parameters constant.

To solve this problem with precise results, it is necessary to consider the three-body, variational problem with optimum staging. In order to avoid the complex calculations involved with such a problem, three assumptions were made: (1) the chemical escape assumption - the chemical stage is fired until at least escape velocity is attained, (2) the two-body assumption - the gravitational effect of the Sun is negligible during the chemical stage flight, while the gravitational effect of the Earth is negligible during the electric stage flight, and (3) the zero time assumption - the time elapsed between chemical stage burnout and sphere of influence penetration is negligible so that electric propulsion commences at the Earth's sphere of influence in heliocentric space. The two-body assumption cannot be realistically made unless the chemical escape assumption already holds. Although some accuracy is lost due to the two-body and zero time assumptions, the main drawback is that chemical stage burnout velocities less than escape velocity are not allowed (chemical escape assumption). Nevertheless, it is felt that adequate results should be obtained, particularly, when high burnout velocities are found to be optimum.

The thrust vector control of the heliocentric phase is determined by variational principles. This means that (1) the Euler-Lagrange equations are employed for the determination of the electric thrustor orientation, (2) the transversality relations are used to optimize the heliocentric travel angle and Earth escape velocity orientation, and (3) the coast phases are optimized.

The payload equation for the chemical-electric hybrid system just described may be written

$$\frac{m_L}{M_o} = \frac{m_o}{M_o}\left(1 - \frac{m_p}{m_o} - \frac{m_{pp}}{m_o} - \frac{m_t}{m_o} - \frac{m_s}{m_o}\right) \tag{1}$$

where m_o/M_o is the payload ratio of the chemical stage and the sum of terms enclosed in parentheses represents the payload ratio of the electric stage. (All symbols are defined in the appendix.) In order to facilitate the discussion concerning the maximization of the payload ratio m_L/M_o equation (1) will be rewritten in terms of the pertinent problem variables (specific impulse, initial acceleration, etc.).

The tankage mass of the electric stage m_t is usually taken to be proportional to the propellant mass of the electric stage m_p. Thus, if k is the proportionality constant,

$$m_t = km_p \tag{2}$$

Defining the specific powerplant mass α to be the ratio of the powerplant mass divided by the power supplied to the thrustors P and defining the thrustor efficiency η to be the ratio of the propulsive power divided by the total power supplied to the thrustors result in the powerplant mass fraction being rewritten as

$$\frac{m_{pp}}{m_o} = \frac{P}{m_o}\,\alpha = \frac{a_o I_e g_o}{47.47\times10^3}\,\frac{\alpha}{\eta} \tag{3}$$

where a_o is the initial acceleration of the electric stage, I_e is the specific impulse of the electric stage, and 47.47×10^3 is a constant that is required for the system of units employed in this report.

The payload mass of the chemical stage (initial mass of the electric stage) can be written as

$$m_o = M_o - M_p - M_h$$

where the hardware mass M_h is composed of such things as tankage mass, engine mass, guidance and control mass, and structure mass. For chemical rockets, the hardware mass can usually be taken to be proportional to the propellant mass M_p. If K is the hardware proportionality constant, then

$$M_h = KM_p \tag{4}$$

Assuming that the chemical stage imparts an impulsive velocity change from circular

orbit velocity V_c to burnout velocity V_b the chemical stage payload ratio is given by

$$\frac{m_o}{M_o} = (1 + K)\, e^{-(V_b - V_c)/I_c g_o} - K \tag{5}$$

If equations (2) to (5) are substituted into equation (1) along with the final mass relation $m_f = m_o - m_p$, there results

$$\frac{m_L}{M_o} = \left[(1 + K)e^{-(V_b - V_c)/I_c g_o} - K\right]\left[(1 + k)\frac{m_f}{m_o} - \frac{a_o I_e g_o}{47.47 \times 10^3}\frac{\alpha}{\eta} - \left(k + \frac{m_s}{m_o}\right)\right] \tag{6}$$

This is the final form of the function to be maximized. The constants in this equation must be ascribed values and these are given in table I. The electric stage final mass ratio m_f/m_o increases as a_o, I_e, and V_b are increased. However, increases in a_o and I_e also increase m_{pp}/m_o, while increasing V_b decreases m_o/M_o. Clearly, there exist values of a_o, I_e, and V_b that will result in a maximum payload ratio. These three variables may be optimized by a three-dimensional search scheme.

The maximization of m_f/m_o can be formulated as a Mayer problem in the calculus of variations wherein mission time is treated as a parameter and the constraints are composed of the two-dimensional equations of motion plus the constraint requiring the thrust magnitude to be either zero or some constant value. This problem has been treated often in the past and its solution is given in reference 9. In the problem at hand, the heliocentric travel angle is left unspecified (free for optimization). Another boundary condition that is not completely specified is the initial heliocentric velocity V_o, which is obtained by vectorially adding the velocity relative to the Earth at the sphere of influence V_s to the Earth's orbit velocity about the Sun $V_\oplus$ as shown in sketches (a) and (b). The optimum orientation of V_s is in the direction of the initial electric thrust vector as can be shown by the transversality condition of the Mayer formulation. The magnitude of V_s is related to the burnout velocity V_b by the conservation of energy as follows:

$$V_s = \sqrt{V_b^2 - 2V_c^2\left(1 - \frac{r_o}{r_s}\right)} \tag{7}$$

TABLE I. - ASSUMED CONSTANTS

Parameter	Assumed value
Circular Earth-orbit velocity, V_c, ft/sec	25 600
Specific impulse of chemical stage, I_c, sec	420
Hardware fraction of chemical stage, K	0.137
Ratio of tankage to propellant mass of electric stage, k	0.02
Ratio of structure to initial mass of electric stage, m_s/m_o	0.04

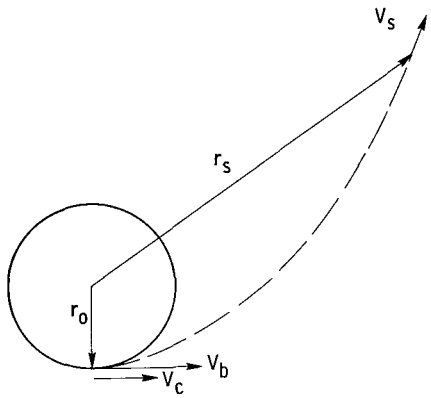

(a) Earth-centered escape maneuver.

(b) Heliocentric initial velocity V_0.

For this study, the sphere-of-influence radius r_s was taken to be 120 Earth radii.

Finally, the specific powerplant mass α and thrustor efficiency η must be considered. Payload ratio is a monotonic function of α; hence, α can be treated as a parameter. Dealing with the thrustor efficiency is a more difficult problem because it is a function of specific impulse, and the functional relation is dependent upon the type of thrustor employed and its state of development. One approach to this dilemma is to assume some characteristic function $\eta(I_e)$ applicable to a particular thrustor. This obviously leads to results that are dependent on the thrustor choice. Alternatively, the choice of thrustor may be delayed by simply treating the ratio α/η as a parameter instead of α (as in ref. 6). However, this approach ignores the dependence of η on I_e, and therefore does not arrive at the true maximum payload ratio except for a hypothetical, constant-efficiency thrustor. Both of these approaches were tried and are examined in more detail in the RESULTS AND DISCUSSION section. In either case, the payload ratio may be maximized by a three-dimensional search on V_b, a_o, and I_e over the class of optimal heliocentric trajectories for any given pair of mission time and α (or α/η).

Optimization Of V_b

Consider a hypothetical case wherein mission time and α have been chosen, both

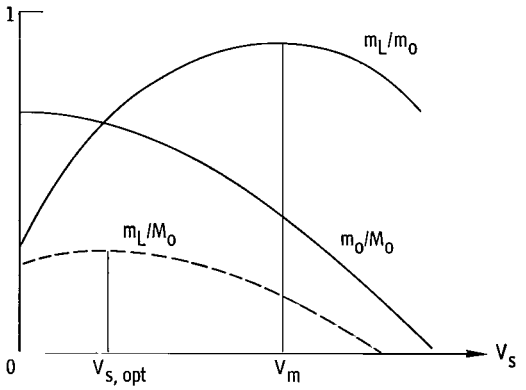

(c) Optimization of V_s for hybrid system.

a_o and I_e have already been optimized, and only V_b remains to be optimized. Since V_b is constrained to take on values at least as large as the escape velocity V_e it might be expected that the optimum V_b could fall exactly on this limit (i.e., $V_{b,\,opt} = V_e$). However, the mathematical model that has been created for the hybrid system ensures that $V_{b,\,opt} > V_e$. That this is so can be easily demonstrated with the aid of sketch (c). In this sketch typical curves of chemical stage payload ratio (m_o/M_o), electric stage payload ratio (m_L/m_o), and overall payload ratio (m_L/M_o) are displayed as functions of the vehicle velocity at the sphere of influence, V_s. For small values of r_o/r_s, the vehicle is considered to have exactly escape energy when $V_s = 0$; hence, from equation (7), the burnout velocity is exactly escape velocity when

$$V_b = V_e = \sqrt{2\left(1 - \frac{r_o}{r_s}\right)}V_c \tag{8}$$

Since $m_L/M_o = (m_o/M_o)(m_L/m_o)$, the slope of the overall payload ratio curve is

$$\frac{d\left(\frac{m_L}{M_o}\right)}{dV_s} = \frac{\partial\left(\frac{m_o}{M_o}\right)}{\partial V_s}\frac{m_L}{m_o} + \frac{\partial\left(\frac{m_L}{m_o}\right)}{\partial V_s}\frac{m_o}{M_o} \tag{9}$$

From equations (5) and (7), it is easily shown that the slope of the chemical stage payload ratio curve is

$$\frac{\partial\left(\frac{m_o}{M_o}\right)}{\partial V_s} = -\frac{1+K}{I_c g_o}\frac{V_s}{V_b}\,e^{-(V_b - V_c)/I_c g_o} \tag{10}$$

Thus, when $V_s = 0$, the slope of the chemical stage payload curve vanishes and the slope of the overall payload ratio curve as given by equation (9) becomes

$$\left[\frac{d\left(\frac{m_L}{M_o}\right)}{dV_s}\right]_{V_s=0} = \frac{\partial\left(\frac{m_L}{m_o}\right)}{\partial V_s}\frac{m_o}{M_o} > 0 \tag{11}$$

The greater than zero inequality can be written since $\partial(m_L/m_o)/\partial V_s$ and m_o/M_o are positive for all cases of interest. Hence, when $V_s = 0$ (i.e., $V_b = V_e$), the overall payload ratio curve has a positive slope.

On the other hand, if V_s is large enough, the slope of the electric stage payload ratio curve $\partial(m_L/m_o)/\partial V_s$ is bound to be negative. For such a V_s both terms of equation (9) are negative and hence the overall payload ratio curve has a negative slope. If V_m denotes the value of V_s where $\partial(m_L/m_o)/\partial V_s = 0$, $V_{s,\,opt}$ has been shown to be bounded by,

$$0 < V_{s,\,opt} < V_m \tag{12}$$

and hence an optimum V_b exists for which

$$V_{b,\,opt} > V_e \tag{13}$$

Electric System

The payload maximization scheme for pure electric propulsion trajectories may be performed similarly to the chemical-electric hybrid system scheme. The burnout velocity V_b is not involved so that only two variables (a_o and I_e) need to be optimized by the search process. Optimum Earth-escape trajectories for low-thrust vehicles are very nearly tangential thrust spirals that can be quite accurately computed in closed form (e.g., ref. 10). Thus, only the heliocentric portion of the flight needs to be optimized. In this case, the ratio m_o/M_o in equation (1) is unity, and the Earth-escape spiral propellant mass m_{ps} may be computed after the heliocentric optimization from the following equation (derived in ref. 10):

$$m_{ps} = m_o\gamma(1 - e^{-\nu}) \tag{14}$$

where

$$\nu = \frac{V_c}{I_e g_o} \tag{15}$$

The empirical correction factor γ is taken to be a function of the ratio of a_o to the local gravitational acceleration g and is displayed on figure 1 (reproduced from ref. 10). The time T_1 required to spiral to escape velocity is computed from the propellant mass and propellant flow rate m_{ps} as follows:

$$T_1 = \frac{m_{ps}}{\dot{m}_{ps}} = \gamma(1 - e^{-\nu})\frac{I_e g_o}{a_o} \tag{16}$$

The aforementioned treatment of the electric system optimization implicitly assumes that the initial heliocentric position and velocity are identical with the Earth's heliocentric radius and orbital velocity.

RESULTS AND DISCUSSION

All-Propulsion Constraint

Preliminary data showed that the optimum payload trajectories tended to be nearly all propulsion (only a short terminal coast phase). Furthermore, as will be shown in the section Comparison of thrustor types, trajectories constrained to all propulsion operation resulted in payload ratios that very nearly equalled the payload ratios obtained when coast phases were allowed. Since the all-propulsion constraint leads to significant simplifications of the problem, it was imposed whenever it was appropriate to do so. Two simplifications arise from this constraint: (1) the boundary-value problem associated with the variational problem becomes much less sensitive and therefore the iterative method of solution converges faster, and (2) a_o is no longer a variable that needs to be optimized; instead, it is determined by the associated boundary-value problem.

Payload Ratio

By using the approach described in the ANALYSIS section wherein α/η is treated as a parameter, and with the all-propulsion constraint imposed, payload ratios were calculated and are plotted as a function of mission time and α/η in figures 2(a) (hybrid system) and (b) (electric system). Lines of constant optimum specific impulse are also

shown and are seen to be fairly flat over most of the range of mission times. Moreover, the optimum specific impulses are relatively low (2000 to 4000 sec) for the region of greatest immediate interest - high α/η. The data for the chemical and nuclear systems appearing in figure 2 were taken from reference 7, wherein the payload ratio was taken to be an increasing function of initial spacecraft mass. Hence a small spectrum of payload ratios is represented in figure 2 as bars. The tops of these bars correspond to spacecrafts that could be inserted into earth orbit by Saturn V class boosters. Spacecrafts inserted into earth orbit by Saturn IB class boosters cannot deliver a positive payload ratio and are not represented in figure 2. The payload performance of chemical and nuclear systems is quite unattractive.

To compare the hybrid and electric systems, figure 2 was superimposed as shown in figure 3. For each value of α/η there is a curve for the electric system and another curve for the hybrid systems. These curves intersect at the point where both systems deliver the same amount of payload. The solid curve in figure 3 passes through these intersection points and thus divides the figure into two regions - one in which the electric system offers greater payloads and another in which the hybrid system offers the greater payloads. Typical present and near future powerplant systems fall into the region wherein the hybrid vehicles offer greater payload capability.

The existence of a region in figure 3 where hybrid systems are poorer than all-electric systems is a consequence of the $V_b \geq V_e$ restriction. As defined earlier, the chemical and electric systems are simply limiting cases of the unrestricted chemical-electric hybrid system. That is, the hybrid system degenerates into the electric system as V_b approaches V_c whereas it degenerates into a single-stage chemical system if V_b becomes large enough. Therefore, a plot of payload ratio as a function of chemical stage burnout velocity that incorporates a proper optimization (arbitrary V_b, inclusion of n-body effects, and inclusion of electric propulsion inside the Earth's sphere of influence) might look something like the solid line in sketch (d). The optimized hybrid system (unrestricted) can never yield a payload ratio lower than either the chemical or electric systems since it includes these systems as degenerate cases. However, if the optimization scheme relies on the assumptions of two-body motion and zero electric propulsion within the Earth's sphere of influence and restricts V_b to values greater than Earth-escape velocity, then according to equation (13), an optimum V_b must also occur at some value greater than Earth-escape velocity. This is illustrated by the dashed line in sketch (d). Of course the true optimum V_b can be as low as V_c. It is only when the true optimum lies in the region $V_c < V_{b,\,opt} \leq V_e$ (as depicted in sketch (d) that the hybrid system as treated herein is credited with a payload ratio significantly lower than it ideally could deliver.

One further point, the dashed line representing the approximate solution in sketch (d) suggests that the exact solution may be shaped quite differently than its

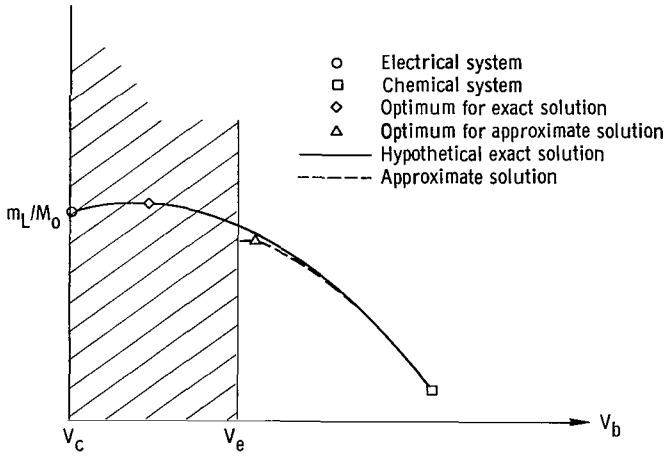

(d) Hybrid system optimization.

representation in this sketch. Indeed, the exact solution may contain an inflection point and perhaps possess two optimums. This question remains unresolved at present, but it is suspected that the inclusion of electric propulsion within the Earth's sphere of influence could remove the $V_{b,\,opt} > V_e$ condition and produce a curve of the shape depicted in sketch (d) for the exact solution.

To compare the electric and hybrid systems for a specific thrustor, it is necessary that the thrustor efficiency be known as a function of specific impulse. Thrustor efficiency data (taken from refs. 11 to 17) is presented in figure 4 for several types of thrustors. As an example, the efficiency function characteristic of small electron-bombardment thrustors with mercury as the propellant was used in conjunction with figure 2 to produce the payload curves shown in figure 5. The sharp changes in the slope of the curves on figure 5 occur because the lower part of each curve represents a restricted ($V_b > V_e$) hybrid system whereas the upper part represents an electric system. That is, for each α only the greatest payload ratio was plotted - regardless of which type of system a particular point belongs. Presumably, if completely arbitrary V_b were allowed for the hybrid system, the payload curves would not suffer a discontinuous slope.

Comparison of optimization schemes. - The payload capability of small electron-bombardment thrustors was also computed using the alternate approach discussed in the ANALYSIS section, that is, treating α as a parameter and including the efficiency curve in the optimization scheme. These results are given in figure 6. The data of figure 5 are reproduced on figure 6 for a direct comparison between the two approaches. The simpler approach, which treats α/η as a parameter, produces payload curves that have the same general shape as the more exact approach. However, in the region of prime interest for the near future - high α and low payload ratio - the error produced by the parametric α/η approach is relatively large. This is because the optimum specific impulses for this region lie on the lower end of the η against I_e curves - where η is a strong function of I_e. Hence, the remaining figures in this report are based on data that include the efficiency curve in the optimization scheme.

Comparison of thrustor types. - In addition to the small electron-bombardment thrustor, two other electric engines were investigated; namely, a large (50-cm diameter) electron-bombardment thrustor and an electrothermal thrustor. The character-

istic efficiency curves for these engines are shown in figure 4. In the case of the electrothermal engine, the tankage fraction was increased to 15 percent since hydrogen is the usual propellant for such engines. The results are shown in figure 7. The gain in efficiency due to increased thrustor size is reflected by a substantial performance increase. The performance of the electrothermal engine is inferior to that of the electron-bombardment engine because of the sizable increase in tankage fraction and unfavorable efficiency curve.

Several cases of optimal coast phase trajectories are also shown in figure 7 for the large electron-bombardment thrustors. It is evident that very little payload benefit results from coasting trajectories - thus justifying the selection of all-propulsion trajectories throughout much of the report.

The optimum specific impulse, high-thrust burnout velocity, and initial power-mass ratio associated with the small size electron-bombardment and electrothermal engines are presented in figures 8 to 10. As a general rule, it can be stated that, as the mission difficulty increases (shorter mission time and/or increased specific powerplant mass), the optimum specific impulse decreases while the optimum high-thrust burnout velocity increases. Figure 10 shows that the hybrid system power requirement is about one-third of the electric system power requirement.

Payload, Power, Mission Time Tradeoffs

Certainly payload is an important parameter to be considered when planning a mission. Other parameters may be of equal importance, however, so that a realistic mission design usually involves a compromise between payload and other factors. One such important factor for the 0.1-AU solar probe mission is the payload power requirement. Nonelectric propulsion system studies must include the mass of a nonpropulsive electric power supply (for telemetry, experiments, etc.) as part of the payload. The "useful payload" is the result of subtracting the power supply mass from the "total payload." The useful payload of electric propulsion systems may be calculated in the same way; however, nonpropulsive power often need not be carried. For instance, during the terminal coast phase associated with optimal flyby trajectories, the power normally available to the electric engines may be available to increase the power available for data transmission and payload experiments. Furthermore, in some cases where propulsive power and nonpropulsive power are needed simultaneously, the nonpropulsive power would cost less than its equivalent for a nonelectric propulsive system. This is because the specific power supply mass of some systems decreases as power is increased and propulsive power is usually many times greater than nonpropulsive power.

In order to illustrate the tradeoff relation between useful payload, power, and

TABLE II. - SYSTEM PERFORMANCE UTILIZING A SATURN IB BOOSTER[a]

System	Mission time, T_M, days	Maximum useful payload, lb	Electric power, kW	Specific impulse, sec	First-stage burnout velocity ft/sec
Chemical rocket (Centaur + "kick" stage)	75	0	0	444, 444	------
Nuclear Rocket (Nerva class)	75	0	0	800, 800	------
Electric rocket[b]	400 to 650	0	--	--------	------
Chemical-electrothermal hybrid[b]	500	850	15	420, 1500	40 000
Chemical - large electron-bombardment hybrid[b]	400 500	1020 2360	35 37	420, 3200 420, 3700	41 000 38 700

[a]Saturn IB assumed to inject 32 000-pound payload into 100-n.-mi. parking orbit.
[b]Specific powerplant mass α = 100 lb/kW.

mission time, these criteria are shown in figure 11 for typical near future systems. All systems were assumed to have been boosted into earth orbit by a Saturn IB and have a specific power supply mass of 100 pounds per kilowatt. The two-stage high performance chemical system data and the one and one-half - stage nuclear system data is presented only at the 75-day mission time since this time represents a minimum energy transfer (i. e., higher mission times are not profitable). Neither of these two systems can deliver positive useful payloads - the negative payloads shown in figure 11 are based on data from an unpublished study by the Advanced Development and Evaluation Division at the Lewis Research Center and reference 7. The pure electric system is also unable to deliver positive payloads and is not represented in figure 11. Thus figure 11 shows that there is no competition among the various systems for this particular case - only the chemical-electric hybrid system can deliver any useful payload. For some other, less difficult missions, there will exist a definite competition between the various systems and a figure similar to figure 11 would display the tradeoffs between useful payload, power, and mission time. In general, high power levels favor the electric and chemical-electric hybrid systems. The important point is that the payload power requirement can strongly influence a system choice in terms of useful payload.

Table II summarizes the results for a Saturn IB booster. It is true that if a larger, more efficient spacecraft were assumed (which could be boosted into Earth orbit by a Saturn V, for example), chemical propulsion alone could deliver some payload (ref. 7) - but by the same token the hybrid system's payloads would increase correspondingly. The nuclear rocket system is similar to the chemical system in that larger boosters are

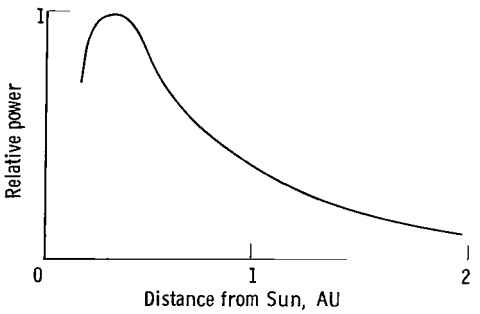

(e) Typical power profile for solar cells.

necessary to provide positive payloads. In addition, nuclear rocket systems do not fall into the near future category. Clearly, if both Saturn V class boosters and nuclear rockets were available, the nuclear-electric hybrid (instead of the chemical-electric hybrid) should be compared to the nuclear system.

Figure 11 and table II illustrate the fact that, while neither the chemical system nor the electric system can accomplish the mission, the hybrid system can. In fact, specific power supply masses on the order of 100 pounds per kilowatt can be realized almost immediately with 5- to 30-kilowatt class solar cell modules (refs. 18 and 19) and 400- to 500-day thrustor lifetimes are reported to be within the present state of the art (ref. 11).

The foregoing analysis has been carried out under the tacit assumption of constant-propulsion power. However, in the case of solar energy dependent power supplies such as solar cell, thermionic, and thermoelectric systems, the power will vary as the distance to the Sun changes unless special means are provided to keep the power constant. This is due to the combined effect of (1) the solar energy flux varying as the inverse square of radius and (2) the power conversion efficiency varying as some function of temperature. Hence, the power profile (power as a function of distance from the Sun, see sketch (e)) of such systems is a complex function involving the type of system and the particular system design as well as the distance from the Sun. In terms of power profiles and specific mass, solar cell power supplies appear more attractive than both thermoelectric and thermionic systems.

One drawback of solar cells is that such a system designed for operation at Earth's radius or greater would experience a sharp power decay between 0.2 and 0.3 AU. While this is not important from a propulsion standpoint (optimum coast phases begin at greater radii), it is quite unfortunate from a payload and communications power standpoint. Thus, a small thermionic generator or thermoelectric panel, whose power output is quite attractive if designed for 0.1-AU operation, might be carried along to supply power to the payload and communication system when the solar cell power output vanishes. Of course, the mass of such a nonpropulsive power supply should be subtracted from the payload to yield useful payload as discussed in the beginning of this section.

The effect of a nonconstant power profile on payload ratio was approximated by computing an average power over the trajectory and using a payload against power plot such as figure 11. If a typical solar cell power profile designed for 1.0-AU operation were assumed, such calculations revealed that, for a 500-day mission employing a 100-pound-

per-kilowatt power supply (α based on 1.0-AU exposure), the payload decrease would be about 20 percent whereas for a 400-day mission with the same power supply the decrease would be about 10 percent. For shorter missions or smaller values of α, the decrease would be less. The existence of an optimum mission time for radius dependent power supply systems (suggested by the previous statements) remains open to question since variational solutions incorporating variable power would modify the constant power trajectories in such a manner that the decrease in payload ratio would be minimized.

Effect of Perihelion Radius

Although one of the basic ground rules for this study is the 0.1-AU perihelion radius requirement, it is of interest to see how changing the perihelion radius affects the solar probe mission. Figure 12 displays the variation of payload ratio as a function of perihelion radius for a hybrid system employing large electron-bombardment thrustors and a 100-pound-per-kilowatt power supply. It is evident that the perihelion radius has a strong effect on payload ratio. However, for mission times on the order of 500 days, perihelion radii of even less than 0.1 AU are readily attainable with the hybrid system.

Trajectory Characteristics

Effect of mission time. - Two typical trajectories of the hybrid system are shown in figure 13. The long mission time trajectories swing far outside Earth's orbit - in fact, for mission times greater than 350 days, a Mars swingby maneuver may be attractive. Arrows denoting thrust direction are placed on the trajectory at equal time increments. It is evident from the trajectory diagram that the long missions are characterized by an initial phase that moves the vehicle into a state of low velocity and a terminal phase which simply removes angular momentum. Figure 13 also shows that long mission time probes have the potential of gathering data over a broader spectrum of solar distances which could at least partially balance the disadvantages of long mission times.

Terminal configuration angle. - An important parameter in communications studies of solar probes is the terminal configuration angle between the Sun-Earth line and the Sun-probe line as shown in figure 14. The Sun is a powerful source of background noise, and there is a communications blackout region when the configuration angle is near 0° or 180°. The terminal configuration angle for the missions employing the small electron-bombardment engines is shown in figure 14.

Absolute and local optimal trajectories. - The bulk of the data presented in this report depends upon the generation of absolute optimum heliocentric trajectories. Such

trajectory calculations can be very difficult since they require solutions to boundary-value problems. Another pitfall is the occasional occurrence of "local optimum" solutions. This is a consequence of the Euler-Lagrange equations being necessary but not sufficient conditions for absolute optimality. During the data generation process, optimum trajectories were encountered in the region of 250- to 350-day missions, which proved to be local optimums rather than absolute optimums. Two optimum trajectories, one local and one absolute, are shown in figure 15 for the same mission. Note that the locally optimum trajectory is characterized by a change from posigrade to retrograde motion. In this study, trajectory solutions that were not absolute optimums were easily identified by this characteristic posigrade-to-retrograde motion and the very poor convergence associated with their boundary-value problems.

Heliocentric ΔV. - In order to facilitate payload computations under weight assumptions different from those assumed in this report, heliocentric characteristic velocity ΔV data is presented in figure 16. Since all-propulsion trajectories are nearly optimum and since ΔV is quite insensitive to specific impulse, figure 16(a) contains all the data that are required for most payload calculations. Appearing as a parameter on figure 16(a) is the velocity relative to the Earth at the sphere of influence V_s, which is related to the chemical stage burnout velocity V_b by equation (7).

The ΔV data shown in figures 16(b) and (c) have been included mainly to illustrate the sensitivity of ΔV with respect to specific impulse and initial acceleration. Figure 16(b) shows that the all-propulsion ΔV is a very weak function of specific impulse for values greater than 3000 seconds. Figure 16(c) indicates that the all-propulsion ΔV is about 30 percent greater than the high acceleration ΔV.

Figure 16(c) also indicates that trajectories with two separate power phases were found to be optimum over a wide range of a_o. These trajectories consisted of an initial power phase, followed by a coast phase, followed by another power phase, and terminated with another coast phase. As a_o is increased, the initial power phase becomes shorter. If a_o is made large enough, the initial power phase vanishes leaving trajectories that commence with a coast phase. Further increases in a_o cause the trajectories to approach the limiting case wherein the power phase is initiated about 75 days (single impulse transfer time) before the end of the mission. Alternatively, instead of holding mission time fixed, mission time could be defined in terms of when a power phase commences (which would eliminate initial coast phases).

CONCLUDING REMARKS

The principal conclusion drawn from this study is that a combination of high-thrust and low-thrust stages can be merged into a hybrid system offering distinct advantages over either system separately. All-chemical systems are quite unattractive for the

close solar probe mission in view of their very small payload ratios. All-electric systems are also unattractive from a payload ratio standpoint unless power supplies having specific powerplant masses (α) of less than 50 pounds per kilowatt become available. But a chemical-electric hybrid system can deliver significant payloads with the relatively high values of α characteristic of present and near future power supplies. For instance, a chemical-electric hybrid system boosted into Earth's orbit by a Saturn IB and employing electron-bombardment engines in conjunction with a 100-pound-per-kilowatt solar cell power supply could deliver a 1000- to 2300-pound useful payload to 0.1 AU - depending upon the mission time.

Consideration of nuclear rocket systems does not alter the essence of the previous remarks. In the first place, an operational nuclear rocket is not in the near future. Of more importance, however, is the fact that if a nuclear rocket were available, then it would be the nuclear-electric hybrid system, which should be compared to the all-nuclear and all-electric systems. Such a nuclear-electric hybrid system should offer the same advantages over the nuclear and electric systems as the chemical-electric hybrid system offers over the chemical and electric systems. Also, because of the nuclear rocket's inherently large size and weight, Saturn V class boosters will be required to insert a 0.1-AU solar probe spacecraft into Earth orbit if reasonable payload ratios are to be attained.

Propulsion system selection is also dependent upon the electric power requirements, a factor that tends to favor electric systems. The chemical-electric hybrid propulsion system calls for intermediate electric power levels - about 30 kilowatt for a 0.1-AU solar probe boosted into Earth orbit by a Saturn IB.

Lewis Research Center,
National Aeronautics and Space Administration,
Cleveland, Ohio, August 30, 1965.

APPENDIX - SYMBOLS

a_o initial acceleration of electric stage, ft/sec^2

g local acceleration of gravity, ft/sec^2

g_o 32.174 ft/sec^2

I_c specific impulse of chemical stage, sec

I_e specific impulse of electric stage, sec

K hardware fraction of chemical stage

k ratio of tankage to propellant mass of electric stage

M_h hardware mass (propellant tanks, engines, structure, etc.) of chemical stage, lb

M_o initial mass of vehicle in circular Earth orbit, lb

M_p propellant mass of chemical stage, lb

m_f final mass, lb

m_L payload mass, lb

m_o initial mass of electric stage, lb

m_p propellant mass of electric stage, lb

m_{pp} powerplant mass of electric stage, lb

m_{ps} propellant mass of Earth-escape spiral, lb

m_s structure mass of electric stage, lb

m_t tankage mass of electric stage, lb

P total power delivered to electric thrustors, kW

r_o initial circular Earth-orbit radius, ft

r_s radius of sphere of influence, ft

T_M mission time, days

T_1 Earth spiral time of electric stage, sec

ΔV heliocentric characteristic velocity, ft/sec

V_b chemical stage burnout velocity, ft/sec

V_c circular Earth-orbit velocity, ft/sec

V_e escape velocity (value of V_b that results in $V_s = 0$), ft/sec

V_o initial heliocentric velocity, ft/sec

V_s velocity at r_s, ft/sec

$V_\oplus$ Earth's heliocentric velocity, ft/sec

α specific mass of electric powerplant, lb/kW

γ correction factor in spiral equations

η thrustor efficiency

θ terminal heliocentric travel angle, deg

ν $V_c/I_e g_o$

φ terminal configuration angle between Sun-probe line and Sun-Earth line, deg

Subscript:

opt optimum

Superscript:

$(\dot{})$ differentiation with respect to time

REFERENCES

1. Athay, R. Grant; and House, Lewis L.: Close in solar Probe. Preliminary Draft Report of Suggested Experiments. NASA TM X-51877, 1963.

2. Matthews, Howard F.; and Erickson, Myles D.: The NASA Advanced Pioneer Mission. Paper 857D, SAE, Apr. 1964.

3. Dugan, Duane W.: A Preliminary Study of the Solar-Probe Mission. NASA TN D-783, 1961.

4. Gobetz, Frank W.: Minimization of Time for Double Impulse Solar Probe Mission. ARS J., vol. 32, no. 3, Mar. 1962, pp. 438-440.

5. Moyer, H. Gardner: Minimum Impulse Coplanar Circle-Ellipse Transfer. AIAA J., vol. 3, no. 4, Apr. 1965, pp. 723-726.

6. Fimple, W. R.; and Edelbaum, T. N.: Applications of SNAP-50 Class Powerplants to Selected Unmanned Electric Propulsion Missions. Paper 64-494, Am. Inst. Aeron. and Astronaut., June 1964.

7. d'Arcy, R. J.; and Sinko, G. C.: Unmanned Electric Propulsion Mission Capabilities of the SNAP-50/SPUR Powerplant. Rep. PWAC-447, Connecticut Aircraft Nuclear Engine Lab., Pratt and Whitney Aircraft Div., United Aircraft Corp., Oct. 1964.

8. Lundholm, J. G., Jr.; Prohaska, E. S.; Hoyer, S.; and Averell, J: A Close Approach Solar Probe Design Feasibility and Mission Study. Paper 64-496, Am. Inst. Aeron. and Astronaut., June 1964.

9. MacKay, John S.; and Rossa, Leonard G.: A Variational Method for the Optimization of Interplanetary Round-Trip Trajectories. NASA TN D-1660, 1963.

10. Melbourne, W. G.: Interplanetary Trajectories and Payload Capabilities of Advanced Propulsion Vehicles. Tech. Rept. 32-68, Jet Propulsion Lab., Calif. Inst. of Tech., Mar. 1961.

11. Mickelsen, William R.; and Kaufman, Harold R.: Status of Electrostatic Thrustors for Space Propulsion: NASA TN D-2172, 1964.

12. Todd, James P.; and Sheets, Ronald E.: Development of a Regeneratively Cooled 30-KW Arcjet Engine. AIAA J., vol. 3, no. 1, Jan. 1965, pp. 122-126.

13. Mickelsen, William R.: Electric Propulsion. Space/Aeronautics, vol. 42, no. 4 Sept. 1964, pp. 50-53.

14. Jack, John R.; Spisz, Ernie W.; and Brinich, Paul F.: Research on Resistance-heated Hydrogen Thrustors. NASA TN D-2281, 1964.

15. Mickelsen, William R.; and MacKay, John S.: Interplanetary Flight with Electric Propulsion. Astronaut. and Aeronaut., vol. 3, no. 1, Jan. 1965, pp. 44-49.

16. Bennett, Stewart; Connors, John F.; and Clark, Kenn E.: Development of a 3-kilowatt Resistojet. Paper 64-672, Am. Inst. Aeron. and Astronaut., Aug. 1964.

17. Reader, Paul D.: Experimental Performance of a 50 Centimeter Diameter Electron-Bombardment Ion Rocket. Paper 64-689, Am. Inst. Aeron. and Astronaut., Aug. 1964

18. Ray, Kenneth A.; and Winicur, Daniel H.: A Large Area Solar Cell Array. Paper 64-739, Am. Inst. Aeron. and Astronaut., Sept. 1964.

19. Gordon, Gary D.: A 30 KW Power Supply from Thin Film Solar Cells. Paper 64-740, Am. Inst. Aeron. and Astronaut., Sept. 1964.

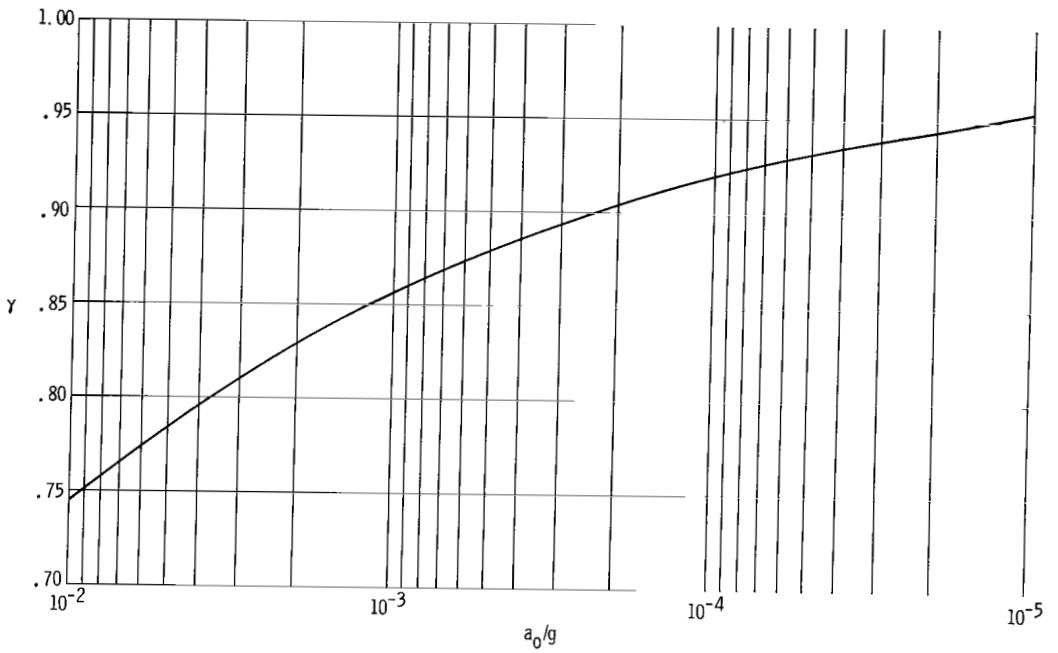

Figure 1. - Correction factor γ for constant-thrust spiral approximations.

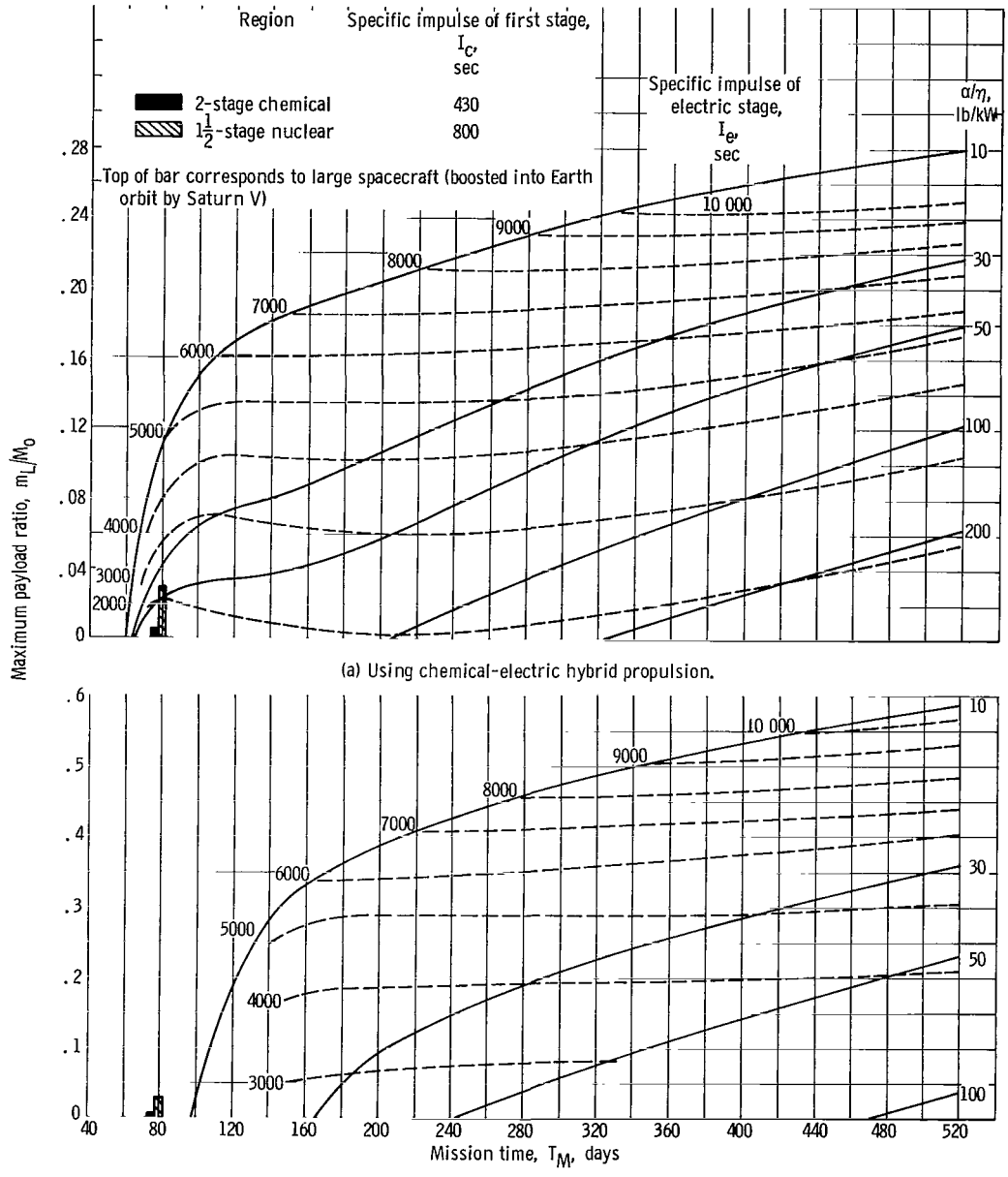

(a) Using chemical-electric hybrid propulsion.

(b) Using electric propulsion.

Figure 2. - Maximum payload ratio for 0.1-AU solar probe. Optimization of payload ratio performed with α/η held constant.

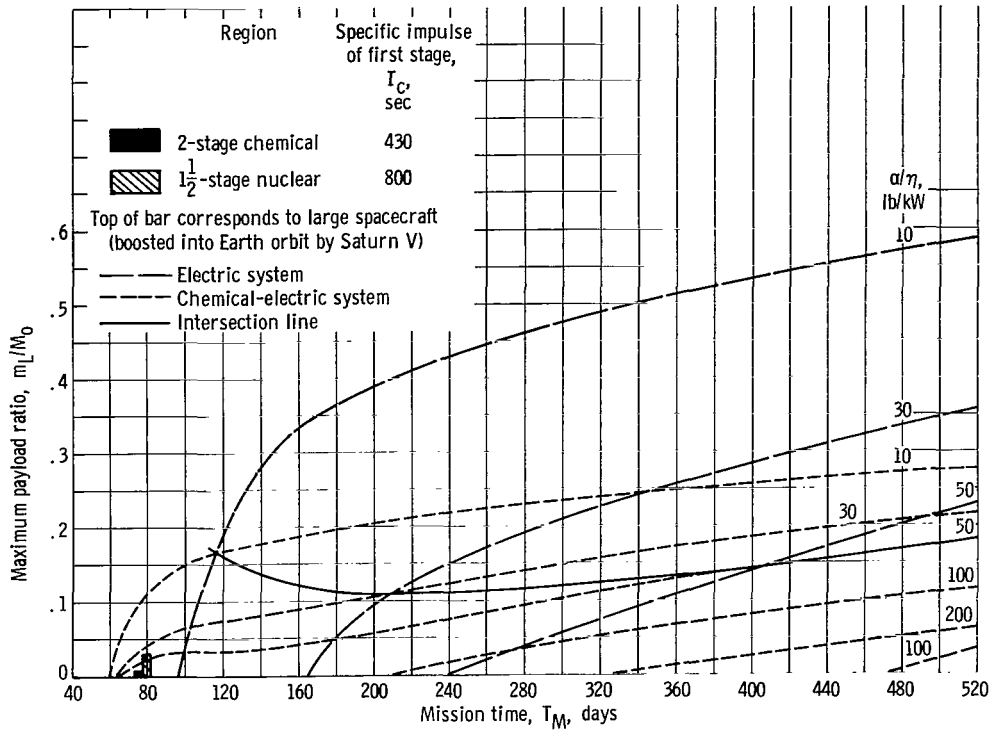

Figure 3. - Comparison between electric system and chemical-electric hybrid system for 0.1-AU solar probe.

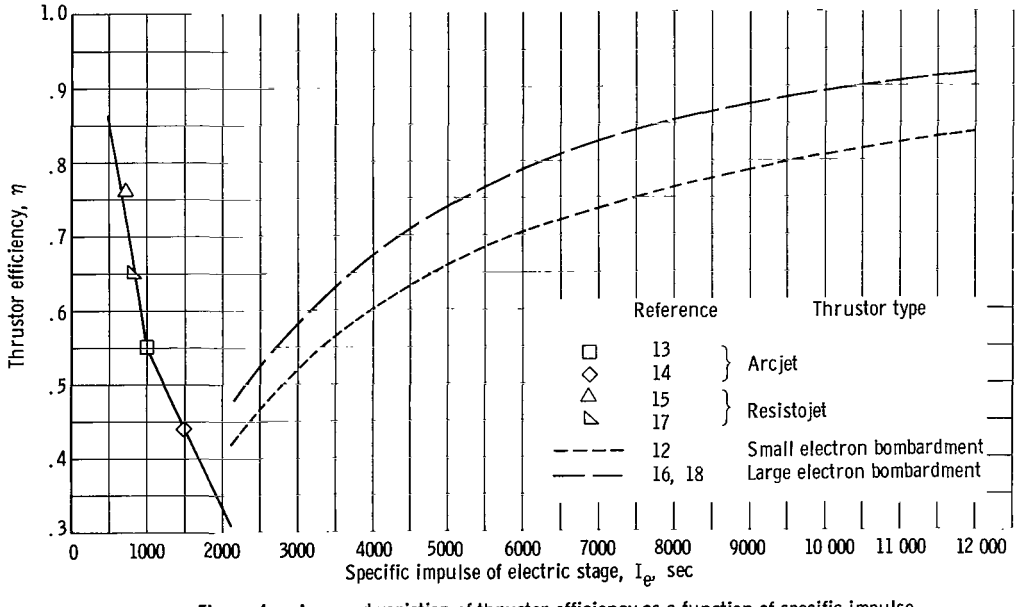

Figure 4. - Assumed variation of thrustor efficiency as a function of specific impulse.

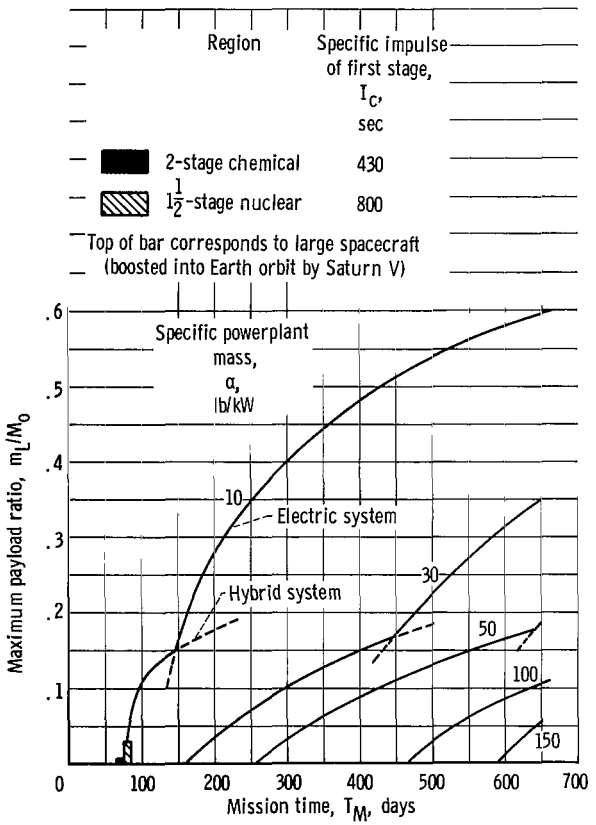

Figure 5. - Maximum payload ratio for 0.1-AU solar probe using small electron-bombardment thrustors. Optimization ignores variation of thrustor efficiency with specific impulse.

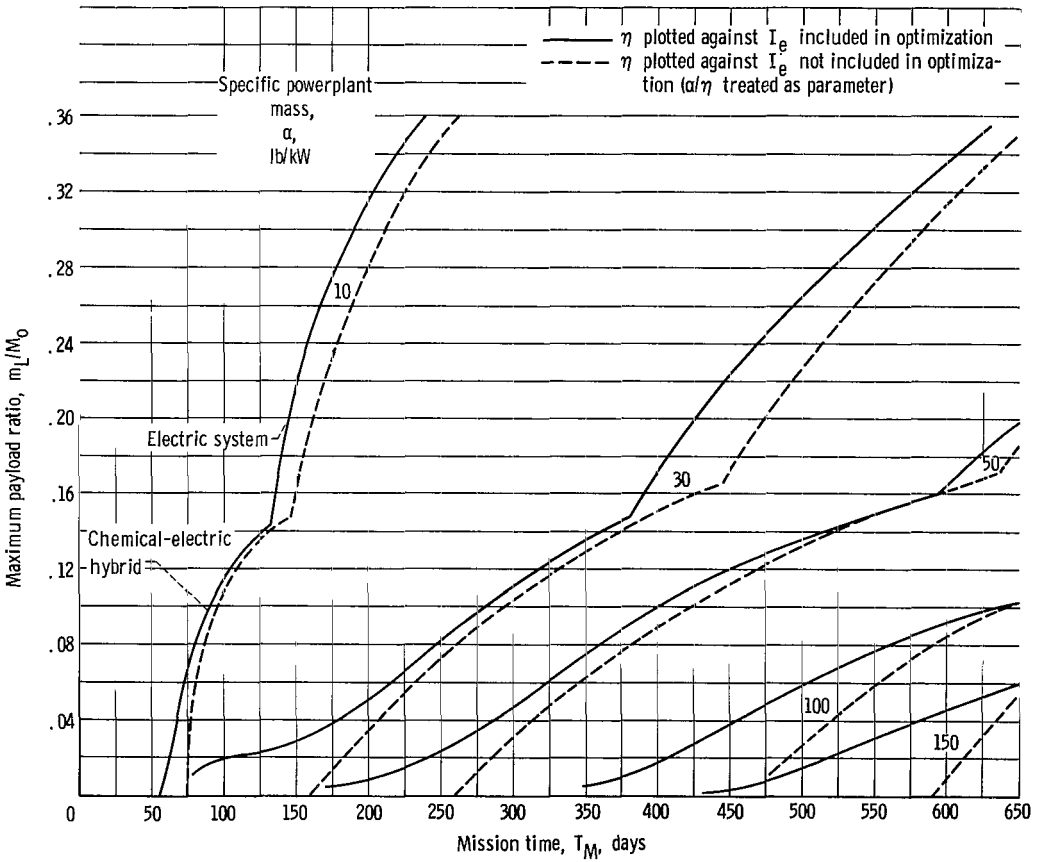

Figure 6. - Comparison of optimization methods using small electron-bombardment thrustors for 0.1-AU solar probe.

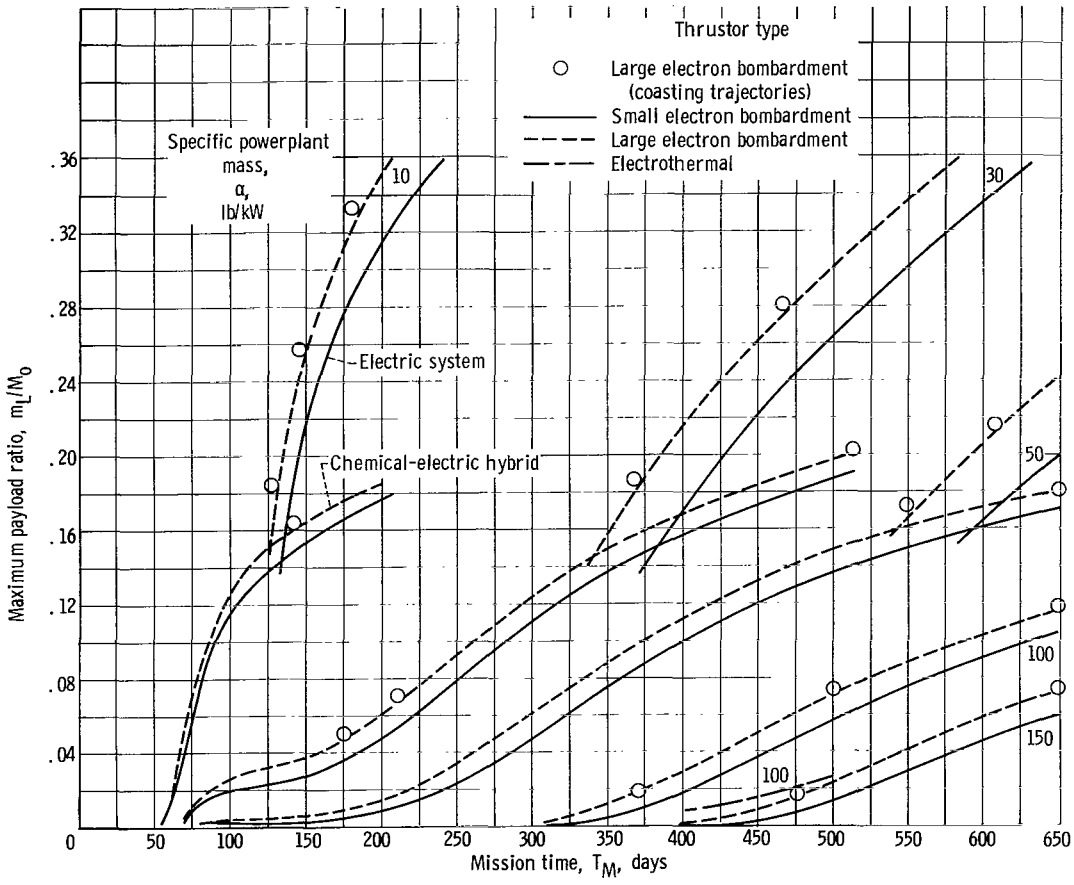

Figure 7. - Maximum payload ratio delivered to 0.1 AU. Optimization includes thrustor efficiency plotted against specific impulse function.

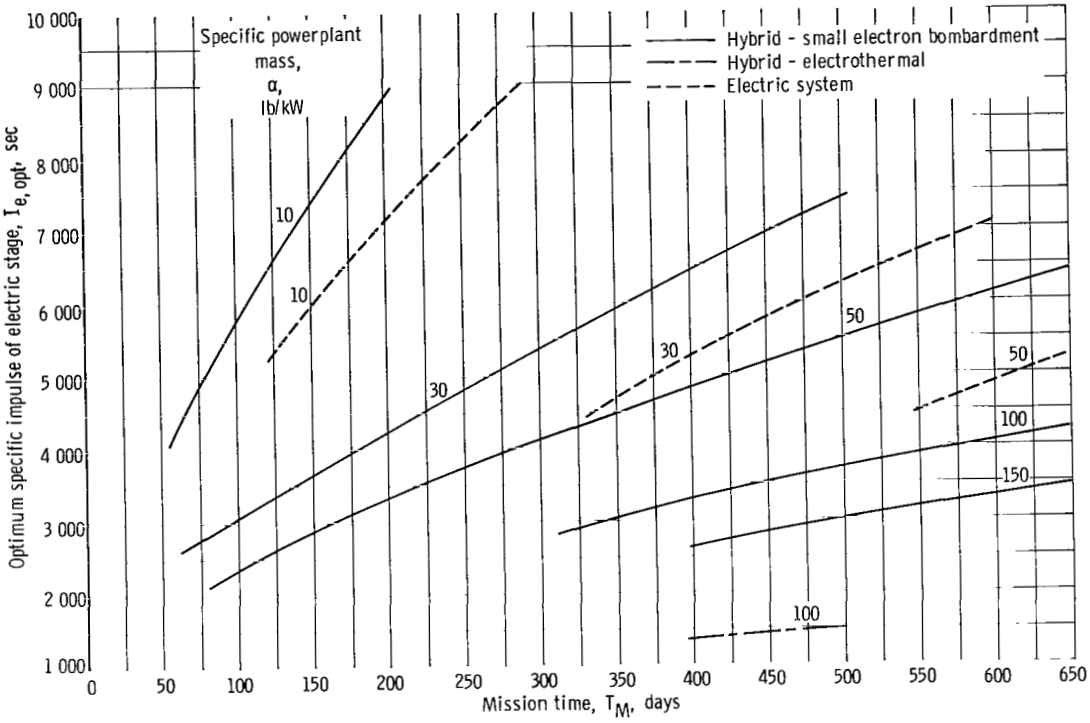

Figure 8. - Optimum specific impulse for 0.1-AU solar probe.

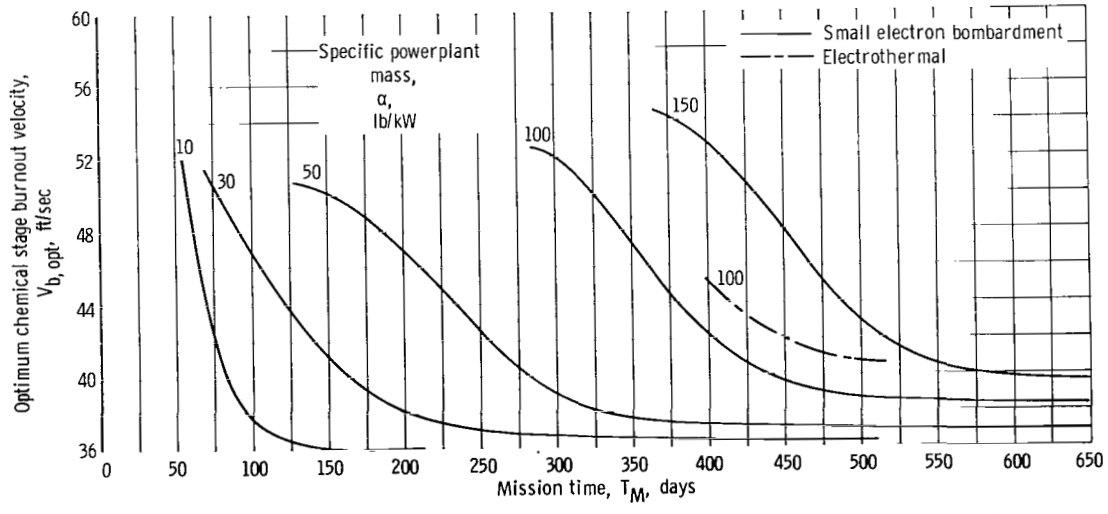

Figure 9. - Optimum chemical stage burnout velocity for 0.1-AU solar probe powered by hybrid system.

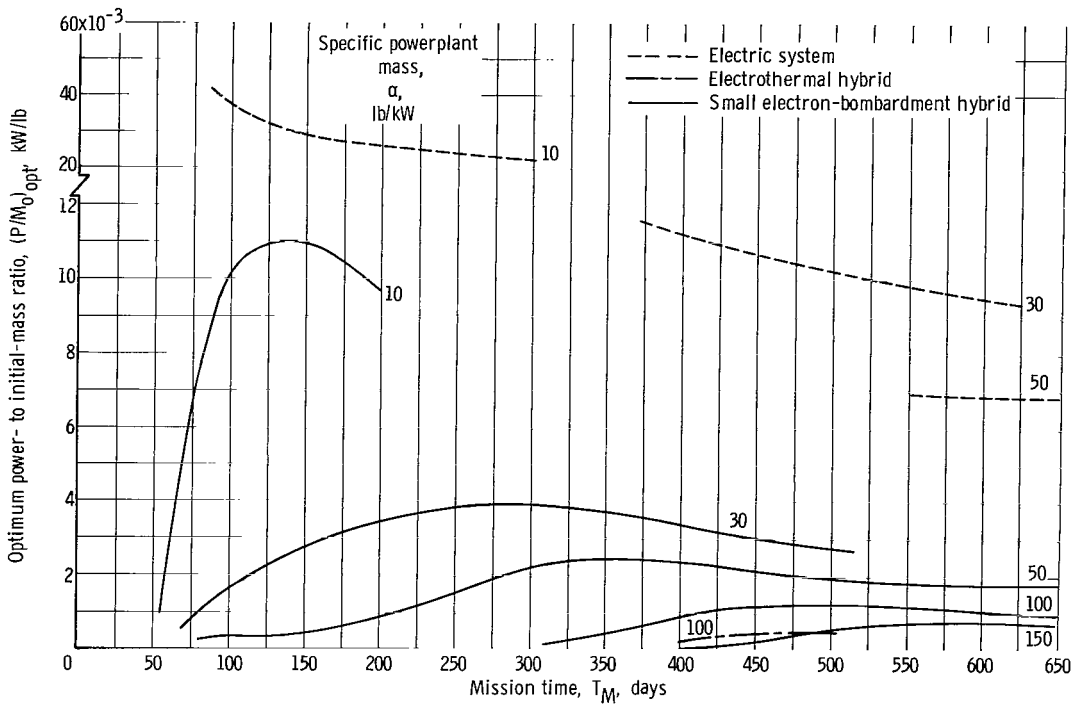

Figure 10. - Optimum power- to initial-mass ratio for 0.1-AU solar probe.

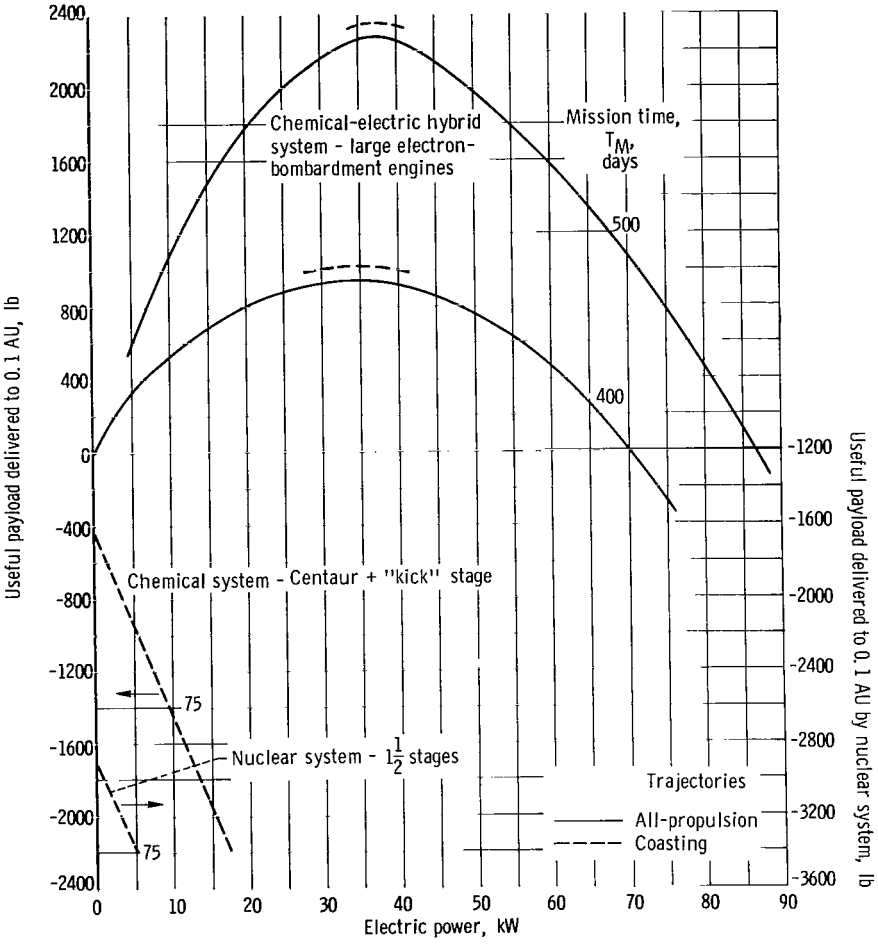

Figure 11. - System performance in terms of useful payload, electric power, and mission time. Specific powerplant mass, 100 pounds per kilowatt; initial mass of vehicle in circular Earth orbit, 32 000 pounds. All systems initially boosted into 100-nautical-mile Earth orbit by Saturn IB.

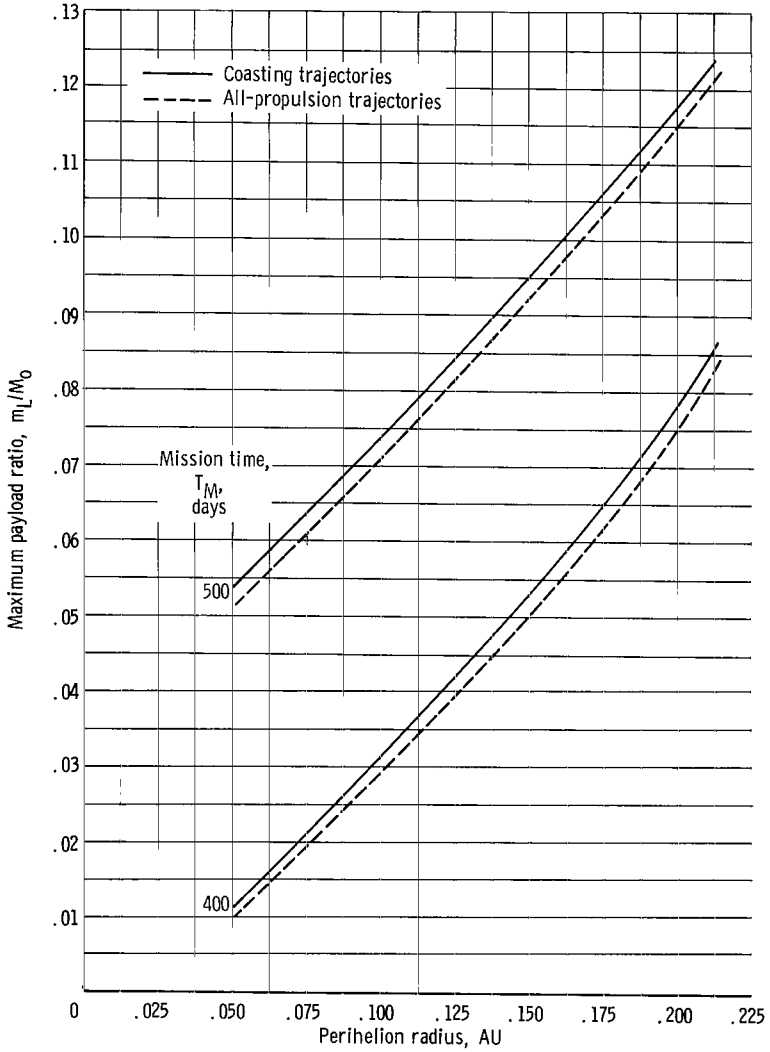

Figure 12. - Effect of perihelion radius for solar probe. Hybrid system with large electron-bombardment thrustors and 100-pound-per-kilowatt power supply.

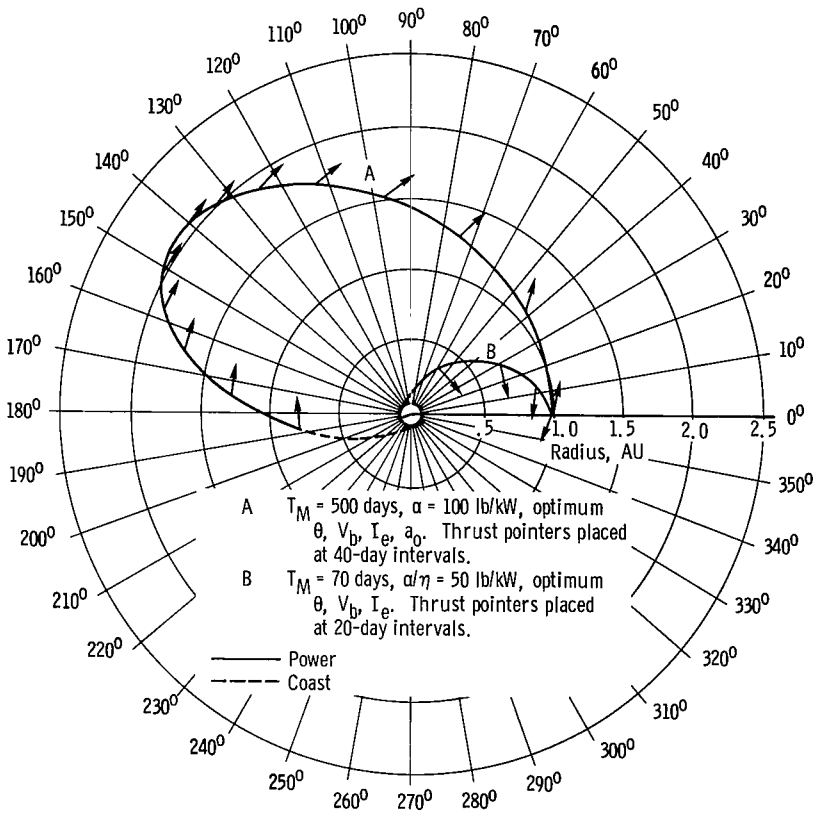

Figure 13. - Trajectory diagrams of two hybrid system missions.

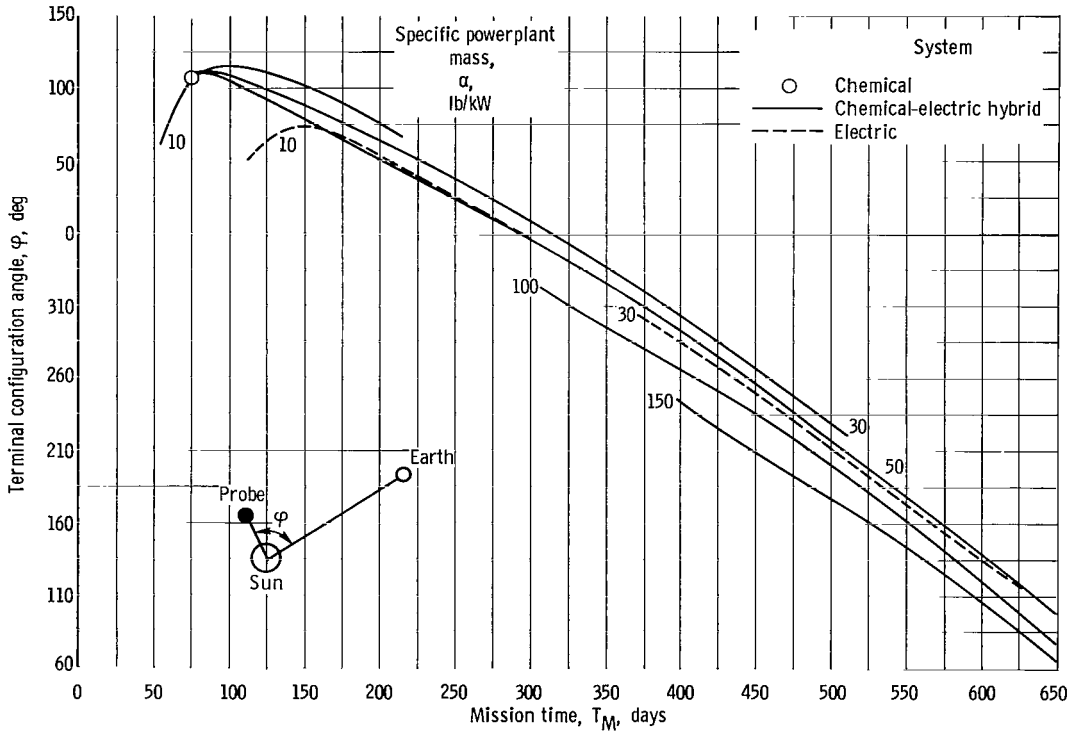

Figure 14. - Terminal configuration angle between Sun-probe line and Sun-Earth line.

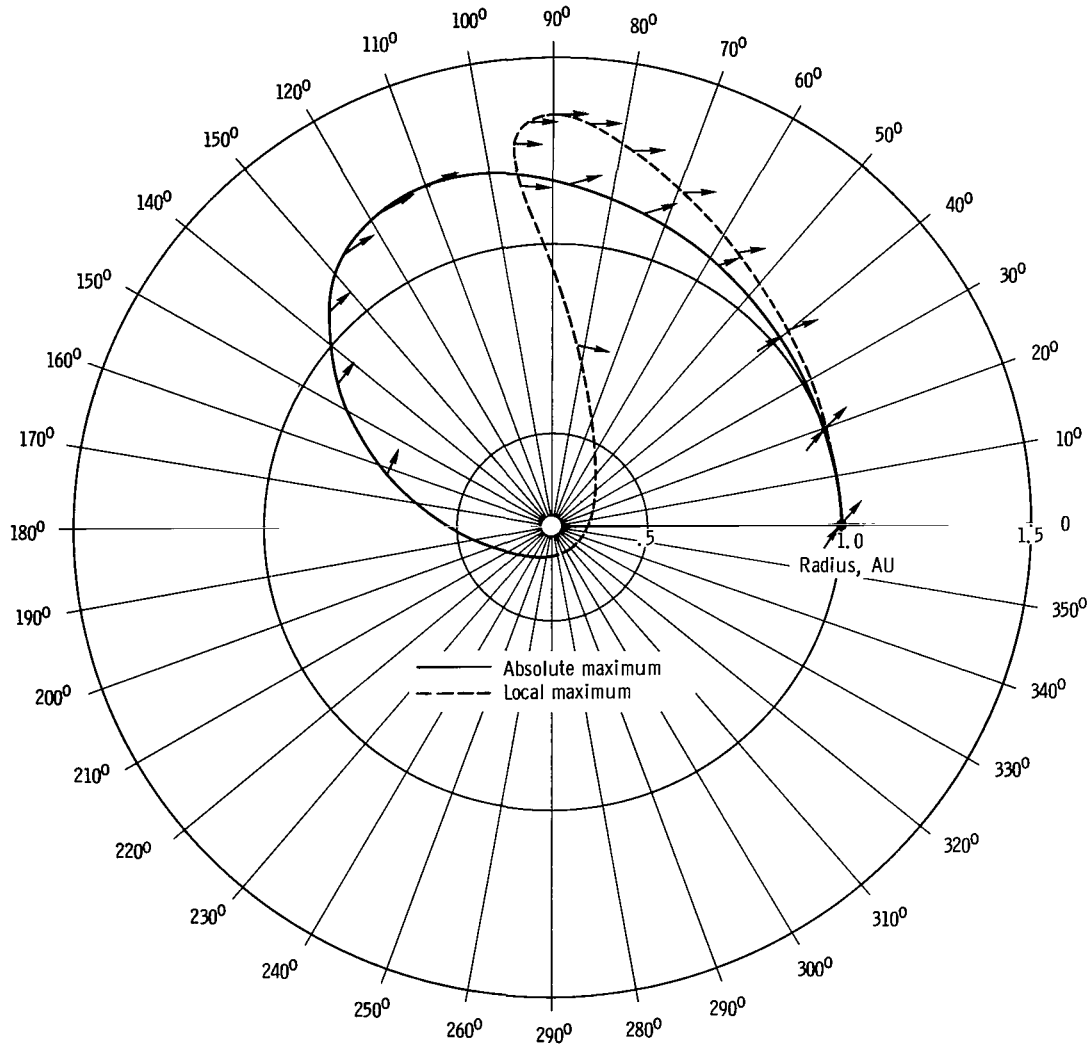

Figure 15. - Trajectory diagram of absolute and local maximums. Mission time, 260 days; specific impulse of electric stage, 8987; optimum travel angle; all-propulsion electric system. Thrust pointers are placed at 20-day intervals.

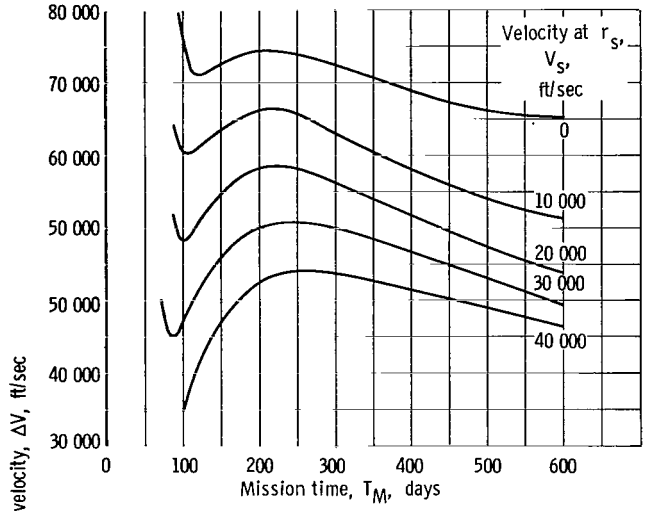

(a) All-propulsion trajectories. Specific impulse of electric stage, 10 000 seconds.

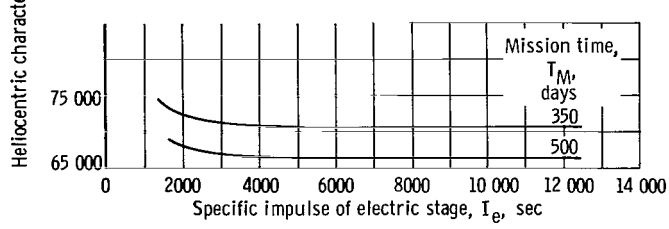

(b) All-propulsion trajectories.

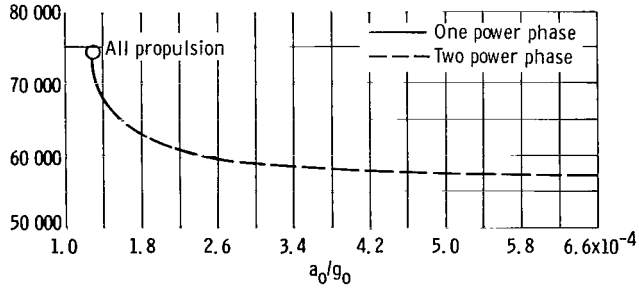

(c) Mission time, 182.5 days; specific impulse of electric stage, 10 000 seconds; velocity at r_s, 0.

Figure 16. - Heliocentric ΔV data.

"The aeronautical and space activities of the United States shall be conducted so as to contribute . . . to the expansion of human knowledge of phenomena in the atmosphere and space. The Administration shall provide for the widest practicable and appropriate dissemination of information concerning its activities and the results thereof."

—NATIONAL AERONAUTICS AND SPACE ACT OF 1958

NASA SCIENTIFIC AND TECHNICAL PUBLICATIONS

TECHNICAL REPORTS: Scientific and technical information considered important, complete, and a lasting contribution to existing knowledge.

TECHNICAL NOTES: Information less broad in scope but nevertheless of importance as a contribution to existing knowledge.

TECHNICAL MEMORANDUMS: Information receiving limited distribution because of preliminary data, security classification, or other reasons.

CONTRACTOR REPORTS: Technical information generated in connection with a NASA contract or grant and released under NASA auspices.

TECHNICAL TRANSLATIONS: Information published in a foreign language considered to merit NASA distribution in English.

TECHNICAL REPRINTS: Information derived from NASA activities and initially published in the form of journal articles.

SPECIAL PUBLICATIONS: Information derived from or of value to NASA activities but not necessarily reporting the results of individual NASA-programmed scientific efforts. Publications include conference proceedings, monographs, data compilations, handbooks, sourcebooks, and special bibliographies.

Details on the availability of these publications may be obtained from:

SCIENTIFIC AND TECHNICAL INFORMATION DIVISION

NATIONAL AERONAUTICS AND SPACE ADMINISTRATION

Washington, D.C. 20546